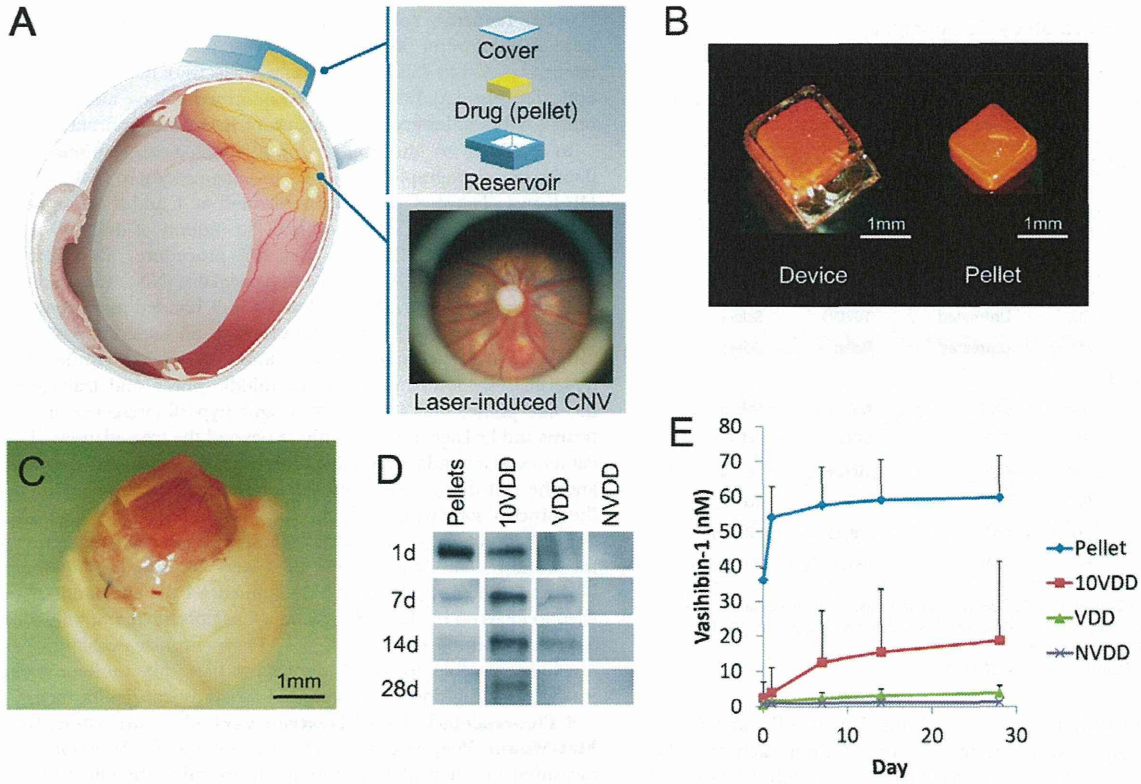

Figure 1. Device and vasohibin-1 release. (A) Schematic image of transscleral sustained vasohibin-1 delivery. We evaluated its effects via transscleral approach for rat laser-induced choroidal neovascularization (CNV). The device consists of a drug pelletized with PEGDM, a reservoir made of TEGDM, and a controlled-release membrane made of PEGDM that contains collagen microparticles. (B) Photograph showing a drug pellet and the delivery device containing a drug pellet. (C) Image of a device placed on the sclera of a rat eye at 3 days after implantation. The amount of vasohibin-1 in the PBS was measured at 1, 7, 14, and 28 days after starting incubation. The representative results of western blotting and the result of ELISA are shown in (D) and (E), respectively. We collected the samples at only the given time points and replaced only the equal volume of PBS. The released vasohibin-1 amounts accumulated for 6, 7, and 14 days. [The pellet samples collected at Day 1 (shown as 1d) were diluted five times due to their concentration before they were evaluated by western blotting]. NVDD: non-vasohibin-1 (vehicle) delivery device, VDD: 1 μM vasohibin-1 delivery device, 10VDD: 10 μM vasohibin-1 delivery device, Pellets: vasohibin-1 pelletized at the same concentration of 10VDD (without reservoir and cover).
doi:10.1371/journal.pone.0058580.g001

injection of ketamine hydrochloride (35 mg/kg) and xylazine hydrochloride (5 mg/kg), and the animals' pupils were dilated with topical 2.5% phenylephrine and 1% tropicamide. Oxybuprocaine hydrochloride (0.4%) was also used for local anesthesia. In all *in vivo* experiments, the animal's left eye was used as a control.

2 Implantation of VDDs, Pellets, and Intravitreal Vasohibin-1 Injection. Devices were implanted subconjunctively in the right eyes of the rats (Table 1). A 4-mm long conjunctival incision was made along the limbus in the upper temporal position. The devices were inserted into the subconjunctival space using forceps, with the drug-releasing surface facing the sclera. The device was placed between the optic disc and the equator, in the posterior quadrant, using no suture to anchor it into place. The conjunctival incision was closed with 9–0 silk and antibiotic ointment was applied to the eyes. Vasohibin-1 protein (0.24 μM) was injected using a 10-μL glass syringe (Hamilton; Reno, NV) 4 days after the experimental CNV procedure. The left eyes were used as untreated controls.

The rats were anesthetized, pupils were dilated, and a fundus examination was performed immediately after the surgery.

Experiment 1: Monitoring the Implanted Devices and Pellets

To monitor the device and drug release, fluorescein isothiocyanate (FITC) dextran (FD40; Sigma-Aldrich) pelletized with PEGDM was prepared and used as a control drug. The FD40 was dissolved in PBS at a concentration of 250 mg/mL and loaded in the device in the same way as vasohibin-1. Eight SD rats were included in this experiment; 4 rats received the FD40 delivery device (FD40DD) and 4 rats received only pelletized FD40.

Experiment 2: Immunohistochemistry after Device Implantation

Immunostaining for vasohibin-1was performed 2 weeks after device implantation. Twelve SD rats were used as follows (Table 1): 4 rats received vehicle (non-vasohibin-1) in the delivery device on the sclera (NVDD), 4 rats received 1.5 μL of 10 μM vasohibin-1 in the delivery device (10VDD), and 4 rats received 1.5 μL of 10 μM vasohibin-1 pellets implanted on the sclera. Immunohistochemistry was performed as reported previously [25].

Animals were euthanized using overdoses of ketamine hydrochloride and xylazine hydrochloride. The eyes were enucleated

Table 1. In Vivo Study Demographics.

Number of animals	Strain	Treatment	Methods	Position of implant
Experiment 1				
4	SD	Untreated	FD40DD	Sclera
4	SD	Untreated	FD40 Pellet	Sclera
Experiment 2				
4	SD	Untreated	NVDD	Sclera
4	SD	Untreated	10VDD	Sclera
4	SD	Untreated	Pellet	Sclera
Experiment 3				
6	BD	CNV	NVDD	Sclera
6	BD	CNV	VDD	Sclera
6	BD	CNV	10VDD	Sclera
6	BD	CNV	Pellet	Sclera
6	BD	CNV	Vehicle	Vitreous
6	BD	CNV	Vasohibin-1	Vitreous

SD: Sprague-Dawley rats, BN: Brown Norway rats, CNV: choroidal neovascularization, NVDD: non-vasohibin-1 delivery device, 10VDD: 10 μM vasohibin-1 delivery device.

doi:10.1371/journal.pone.0058580.t001

and fixed for 12 hours in 4% paraformaldehyde (PFA) at 4°C. The anterior segment and lens were removed from each eye. The posterior segment was cryoprotected at 4°C through successive 12-hour incubations in 10%, 20%, and 30% sucrose dissolved in saline. The tissues were immersed in OCT compound (Tissue-Tec; Sakura Finetec USA, Inc., Torrance, CA, USA) and frozen in acetone in a dry-ice bath. The frozen posterior segment was sectioned at the center of the implanted area at a thickness of 5 μm for each section, using a cryostat. We examined eight continuous sections per eye. The sections were incubated in rabbit polyclonal antibody against human vasohibin-1, followed by FITC-conjugated anti-rabbit IgG (1:200; Dako, Glostrup, Denmark) for 30 minutes. The sections were washed three times with PBS between each step. Negative controls (4 rats) incubated with just FITC-conjugated anti-rabbit IgG were also prepared. Slides were counterstained with 4, 6-diamino-1-phenylindole (DAPI; Vector Laboratories, Burlingame, CA, USA) and photographed using a fluorescence microscope (Leica FW4000, Ver. 1.2.1; Leica Microsystems Japan, Tokyo, Japan).

Experiment 3: Choroidal Neovascularization Study

A total of 36 BN rats were used (Table 1). The devices and pellets were implanted on the same day as the CNV procedure. The rats were divided into six groups (6 rats in each group): rats with NVDD, rats with 1.5 μL of 1 μM vasohibin-1 in the delivery device (VDD), rats with 1.5 μL of 10 μM vasohibin-1 in the delivery device (10VDD), rats with 1.5 μL of 10 μM vasohibin-1 pellets implanted on the sclera, rats with intravitreal injection of 5 μL of vehicle, and rats with an intravitreal injection of 0.24 μM vasohibin-1 protein occurring 4 days after the experimental CNV procedure. The amount of intravitreal vasohibin-1 used and the day of the injection were determined based on our previous data [25]. The intravitreal injections were performed using a 10-μL glass syringe (Hamilton), and the needle was passed through the sclera just behind the limbus into the vitreous cavity.

3 CNV procedure. A green argon laser was used to rupture the choroidal membrane using a slit-lamp delivery system (Ultima 2000SE; Lumenis, Yokneam, Israel) with a contact lens [31]. The laser settings were: 50 μm diameter for 0.1 sec duration, at an intensity of 650 to 750 mW. Six laser burns were made around the optic disc (Fig. 1A). Each burn was confirmed to have induced subretinal bubbles, indicating a rupture of Bruch's membrane.

In addition to the routine ophthalmological examinations, fluorescein angiography (FA) with an imaging system (GENESIS-Df; Kowa, Tokyo, Japan) was performed at 1 and 2 weeks after the CNV laser burn, and choroidal flat mounts of the CNV site were performed at 2 weeks after the procedure. Two retinal specialists (HO and TA) and one non-specialist (NN) evaluated the angiograms for FA grading evaluation in a blinded manner using a grading system [32], where Grade 1 = no hyperfluorescence; Grade 2 = hyperfluorescence without leakage; Grade 3 = hyperfluorescence in the early or middle phase and leakage in the late phase; and Grade 4 = bright hyperfluorescence in the transit and leakage in the late phase beyond the treated areas. The camera was a handheld retinal camera for photographing humans, and the fact that rat eye optics differ from that of humans made the process somewhat difficult. Intense fluorescein leakage also made the results of photographs as faint. The laser burn sometimes made subretinal hemorrhages that were shown as fluorescein blockage. These results may have influenced the evaluation. We tried to focus on the laser burn as much as possible to not influence the evaluation. Further we also tried to synchronize evaluations as much as possible to avoid significant bias due to fluorescein leakage. Total grades were analyzed for statistical significance.

4 Fluorescein-Labeled Dextran Perfusion and Choroidal Flat-Mount Preparation. The size of the CNV lesion was measured on choroidal flat mounts to examine the effect of the vasohibin-1 delivery device (n = 6 eyes/group and each eye had 6 laser spots). Fourteen days after the CNV procedure, the rats were perfused with 5 mL PBS containing 50 mg/mL fluorescein-labeled dextran (FITC-dextran, MW: 2×10^6; Sigma-Aldrich). Results of mouse CNV experiments [25] indicated that laser-induced CNV lesions were most active at 14 days after laser application and gradually self-resolved more than 28 days after the laser burn. This data was supported by our previous study of laser-burned monkey eyes [28].

We enucleated the eyes in the current study at 14 days after the CNV laser procedure, after euthanizing the animals per the previously described method. The eyes were removed and fixed for 30 minutes in 4% phosphate-buffered PFA. The cornea and lens were removed and the entire retina was carefully dissected from the eyecup. Radial cuts (4 to 6) were made from the edge to the equator, and the eyecup of the RPE-choroid-sclera (R-C-S) complex was flat mounted in Permalfuor (Beckman Coulter; Fullerton, CA, USA) with the scleral side facing down. Flat mounts were examined by fluorescence microscopy (Leica FW4000, Leica Microsystems Japan), and the total area of each CNV zone associated with each burn was measured. The CNV lesions were identified by the presence of fluorescent blood vessels on the choroidal/retinal interface circumscribed by a region lacking fluorescence. This process duplicated past reported procedures [33,34]. Two retinal specialists (HO and TA) and one non-specialist (NN) evaluated the size of the dextran-fluorescein perfused CNVs in a blinded manner, as described above.

Statistical Analyses

Analysis of variance (ANOVA) with Tukey's test was used to examine differences in the leakage and severity of the CNVs in the fluorescein angiograms and the area of the choroidal flat mount. Endothelial tube formation was also evaluated by this method. P-values less than 0.05 were considered significant.

Results

In Vitro Vasohibin-1 Release from the Device

Each result is shown as mean ± SD of three different experiments in Figure 1E. A prominent initial increase was observed in vasohibin-1 pellets (Pellet) and it appeared to almost plateau at 7 days after the start of incubation. A minor increase was observed in the vasohibin-1 delivery devices (VDD) with an almost level release observed over the 28 days of incubation. If we examine the amount released from the device (4×4×1.5 mm) between Days 7 and 28, the amount released was estimated to be 0.31 nM/day in the 10VDD group, 0.070 nM/day in the VDD group, 0.088 nM/day in the pellets, and 0 in the NVDD group (Fig. 1E) in a closed incubation system, when we used 500 mg/mL COLs for the permeable PEG/COLs membranes. These calculations were performed from the fitting line between 0 and 28 days. In rat experiments, the release amount would be less, because we used a smaller device for rats than used in the *in vitro* release assay. The larger device used in the *in vitro* release assay in Fig. 1E had 5.44 times (12.25 mm^2 vs 2.25 mm^2) larger drug-releasing surface area and 3.42 times faster releasing rate than that of the transplanted device used in rats, from the results of Fig. S1. The total amount of vasohibin-1 released from the 10VDD devices during the CNV suppression experiment in rats was estimated grossly to be approximately 4.28 nM over 2 weeks. The total amount of vasohibin-1 during the 2 weeks was estimated as about 14.6 nM from the results of Figure 1E, and was divided by 3.42, which is the difference in releasing rate between *in vitro* release assay and *in vivo* experiments, although the effective amount of vasohibin-1 in CNV suppression would be smaller than 4.28 nM, due to drug elimination from the eye. These results were confirmed by western blotting analysis; Figure 1D shows the representative results at Days 1, 7, 14, and 28. A greater amount of vasohibin-1 was observed in the 10VDD and pellet groups than was seen in the NVDD and VDD groups. The results of the pellet group at Day 1 (1d in Fig. 1D) was obtained after diluting the samples five times, because the concentration was too high to be shown by western blotting. However, the size of the pellets was much smaller after 7 days of incubation.

Endothelial Tube Formation

Endothelial tube formation of HUVECs cultured on the NHDF layer was assessed using anti-human CD31 immunostaining (Fig. 2). We used a range of native vasohibin-1 concentrations (from 0 to 10 nM, using 2 nM VEGF) for the preliminary experiments. After the initial examination, the cells were fixed and stained using anti-human CD31. Figures 2A–2G show representative photographs of the experimental results. Figure 2E shows the results of released vasohibin-1 (0.56 nM) from the devices with 2 nM VEGF. Figure 2H shows the average of each experiment; significantly fewer CD31-positive points were observed in released vasohibin-1-treated wells when compared to those of the vehicle released from the NVDD ($p = 0.000001$) or VEGF-treated control ($p = 0.000002$). Vasohibin-1 released from the device showed activity comparable to the native vasohibin-1.

Macro Examination

FD40 was detected in the device (Figs. S2A and S2B show color and fluorescein photographs, respectively) or in pellets (Figs. S2G and S2H) at the implant site through the conjunctiva in the live rats. When we enucleated the eyes at a week after device implantation, mild fibrosis was observed around the devices (Fig. S2C) and around the pellets (Fig. S2I). Fluorescein photography demonstrated the presence of FD40 in the device, with little fluorescein in the conjunctiva and surrounding tissues (Fig. S2D, arrow). FD40 was also detected in the sclera after removal of the device (Figs. S2E and S2F, arrow). Conversely, FD40 pellets showed strong fluorescein on the conjunctiva and surrounding tissues, as was seen for the pellet itself (Fig. S2J, arrow). Furthermore, little fluorescein was observed on the sclera after removal of the device (Figs. S2K and S2L, arrow). Similar conditions were observed when we examined the tissues at 2 weeks after device and pellet implantation; fluorescence was observed over a wider area for those specimens where the device was implanted compared to results at Week 1 (data not shown).

Immunohistology of Vasohibin-1

In immunostained eyes, vasohibin-1-positivity was found in only the 10VDD group (Fig. 3B), but not in the NVDD group (Fig. 3A) or the negative control without the first antibody (Fig. 3D), mainly at the region where vasohibin-1 releasing devices were placed. Pellets showed strong local immunoreactivity, but no immunoreactivity in the retina (Fig. 3C). Vasohibin-1 positivity was observed in the neural retina and optic nerve (white arrows in Fig. 3B). Strong immunoreactivity was observed in the choroid, RPE, and at the inner layer (such as the ganglion cell layer [GCL]) by magnified photographs after device implantation (Fig. 3E).

Leakage from CNV

Fluorescein angiography results of each group at 1 week after the laser CNV procedure are shown in Figure 4A. The results show that an intravitreal injection of vasohibin-1 on Day 4 after the CNV procedure led to a significant reduction of FA scores when compared to those of NVDD ($p = 0.00014$), pellet ($p = 0.020$), and vehicle injection ($p = 0.040$) (Fig. 4B). The 10VDD implantation led to a significant reduction of FA scores when compared to the result of the NVDD group ($p = 0.00006$). The VDD implantation led to a significant reduction of FA scores when compared to those of NVDD ($p = 0.000017$), pellet ($p = 0.012$), and vehicle injection ($p = 0.026$). Although FA scores of the 10VDD group seemed to be smaller than those of the pellet ($p = 0.065$) and vehicle injection ($p = 0.12$), the results were not significant. Figure 5A shows the FA results at Week 2 in each group. Significantly lower FA scores were observed for the vasohibin-1 intravitreal injection group when compared to those of NVDD ($p = 0.000022$), and vehicle intravitreal injection ($p = 0.0065$). Further, significantly lower FA scores were observed in the 10VDD group when compared to those of NVDD ($p = 0.000003$) and vehicle injection ($p = 0.0080$) (Fig. 5B). Significantly lower FA scores were also observed in the VDD group when compared to those of NVDD ($p = 0.000058$) and vehicle injection ($p = 0.011$).

Flat-mount Examination of the CNV Site

Choroidal flat mounts were prepared 2 weeks after device implantation; representative results of each group are shown in Figure 6A. The area of the CNV was 27,288±7,975 μm^2 for the NVDD group; 23,532±13,120 μm^2 for the VDD group; 17,382±715 μm^2 for the 10VDD group; 30,502±780 μm^2 for the vasohibin-pellet group; 26,900±9,067 μm^2 for the intravitreal vehicle injection group, and 12,731±4,113 μm^2 for the intravitreal vasohibin-1 injection group (Fig. 6B). The CNV area was smaller in eyes that were treated with 10VDD or intravitreal vasohibin-1 injection compared to the other treatments. A significantly smaller CNV area was observed in the 10VDD group when compared to those of the NVDD ($p = 0.0004$), pellet transplantation ($p = 0.0011$), and intravitreal vehicle injection groups ($p = 0.000015$). A significantly smaller CNV area was also

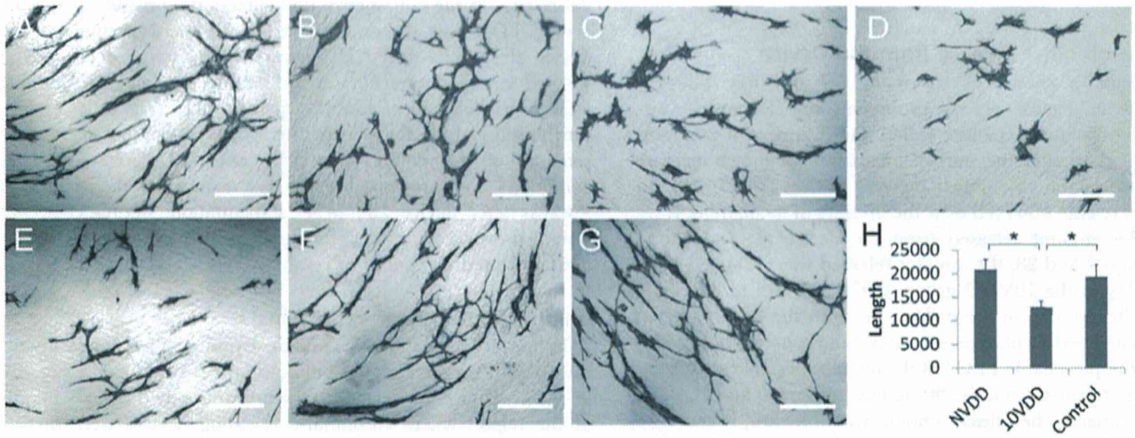

Figure 2. The activity of vasohibin-1 by an endothelial cell tube formation assay. The activity of vasohibin-1 was confirmed by an *in vitro* endothelial cell tube formation assay. Vasohibin-1 suppressed the HUVEC tube formation in a dose-dependent manner. Representative results of HUVEC tube formation treated with 2 nM VEGF combined with 0 (A), 0.2 (B), 2 (C), and 10 nM vasohibin-1 (D) are shown. Bars indicate 100 μm. The released vasohibin-1 from the device showed comparable results to native activity (E). Significant suppression of HUVEC tube formation was observed in released vasohibin-1 when compared to those treated with NVDD (F) and with only 2 nM VEGF without vasohibin-1 (G). (H) shows the average of each experiment; significantly fewer CD31-positive points were observed in released vasohibin-1-treated wells when compared to those of the vehicle released from NVDD ($p<0.0001$) or the VEGF-treated control ($p<0.0001$). The vasohibin-1 released from the device showed activity comparable to the native vasohibin-1. Vertical bar indicates total length of tube formation. NVDD: non-vasohibin-1 (vehicle) delivery device, 10VDD: 10 μM vasohibin-1 delivery device.
doi:10.1371/journal.pone.0058580.g002

observed in eyes injected with intravitreal vasohibin-1 when compared to those of the NVDD ($p = 0.000006$), VDD ($p = 0.0036$), pellet transplantation ($p = 0.000023$), and intravitreal vehicle injection groups ($p = 0.000001$) (Fig. 6B). No significant difference was observed when we compared the VDD with those

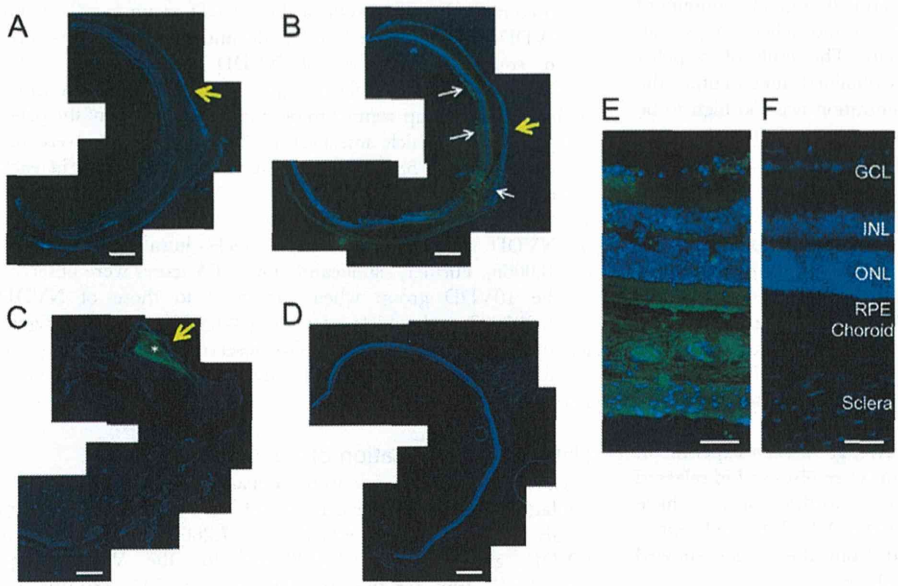

Figure 3. Immunohistochemistry of vasohibin-1 after device implantation. The immunohistochemistry results of vasohibin-1 after NVDD, 10VDD, and pellet implantation are shown. No immunoreactivity was observed after NVDD transplantation (A) and negative control without first antibody (D). 10VDD shows vasohibin-1 immunoreactivity at the device implant area (B). White arrows show the immunoreactivity in the retina and optic nerve at low magnification. Diffuse immunoreactivity was observed in the sclera, choroid, RPE, and retina at greater magnification (E). Strong immunoreactivity was observed in the ganglion cell layer (GCL) and retinal pigment epithelium (RPE), as well as in the sclera and choroid. INL and ONL indicate the inner and outer nuclear layers. These results were not observed in the NVDD group (A) or the negative controls (D and F). Strong immunoreactivity was observed in the pellet (asterisk) and in the tissues surrounding the implanted pellet (C). Yellow arrows indicate the positions where devices or pellets were placed. Devices were removed before sectioning, but pellets were not removed before sectioning. Bars: 200 μm (A–D), and 50 μm (E, F).
doi:10.1371/journal.pone.0058580.g003

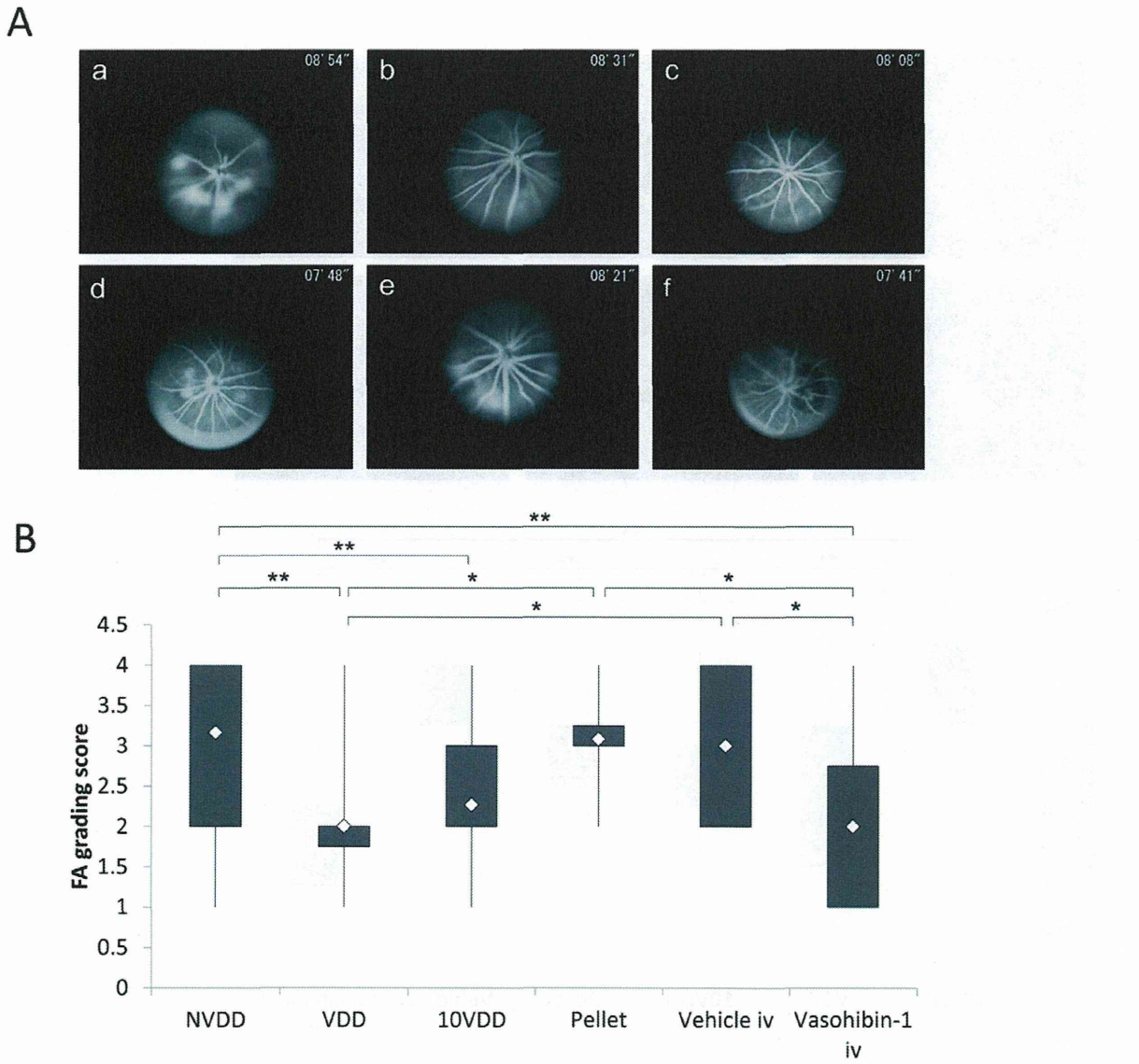

Figure 4. Fluorescein angiography 1 week after CNV laser procedure. (A) Representative results of fluorescein angiography (FA) in each group at 1 week after CNV laser procedure. The groups were treated with NVDD (a), VDD (b), 10VDD (c), vasohibin-1 pellet (d), intravitreal vehicle injection (Vehicle iv) (e), or intravitreal vasohibin-1 injection (Vasohibin-1 iv) (f). (B) Fluorescein angiography scores for each of the six laser spots in each eye are plotted and calculated for each group. Significantly lower FA scores was shown in the Vasohibin-1 iv group when compared to those of NVDD ($p = 0.00014$), pellet ($p = 0.02$), and Vehicle iv ($p = 0.040$). Significantly lower FA scores are also observed in the 10VDD group when compared to the NVDD group ($p = 0.00006$). Significantly lower FA scores are also observed in the VDD group when compared those of NVDD ($p = 0.00017$), Pellet ($p = 0.012$), and intravitreal vasohibin-1 injection ($p = 0.026$). Significant differences are shown as asterisks. NVDD: non-vasohibin-1 (vehicle) delivery device, VDD: 1 μM vasohibin-1 delivery device, 10VDD: 10 μM vasohibin-1 delivery device, Pellet: vasohibin-1 pelletized at the same concentration of 10VDD (without reservoir and cover).
doi:10.1371/journal.pone.0058580.g004

of NVDD ($p = 0.7374$), pellet transplantation ($p = 0.3616$), and intravitreal vehicle injection ($p = 0.7178$) groups.

Discussion

Attention has been paid to sustained drug delivery in the treatment of AMD because regimens including intravitreal anti-VEGF injection require repeated injection and may lead to adverse side effects [9,35]. Sustained delivery of large molecules such as antibodies may be attractive, because not only anti-VEGF therapy and anti-TNFα antibody have shown excellent results in the treatment of refractory eye diseases (such as Behcet's disease), although this regimen also requires repeated cycles of therapy [36,37]. When our devices were cultured in PBS, vasohibin-1 was released over time, with activity equivalent to that seen with native vasohibin-1. These positive results were also observed with brain-derived neurotrophic factor (BDNF) and 40 kDa dextran, as reported previously [24]. Our implantable device showed sustained protein release over time. The relatively large standard

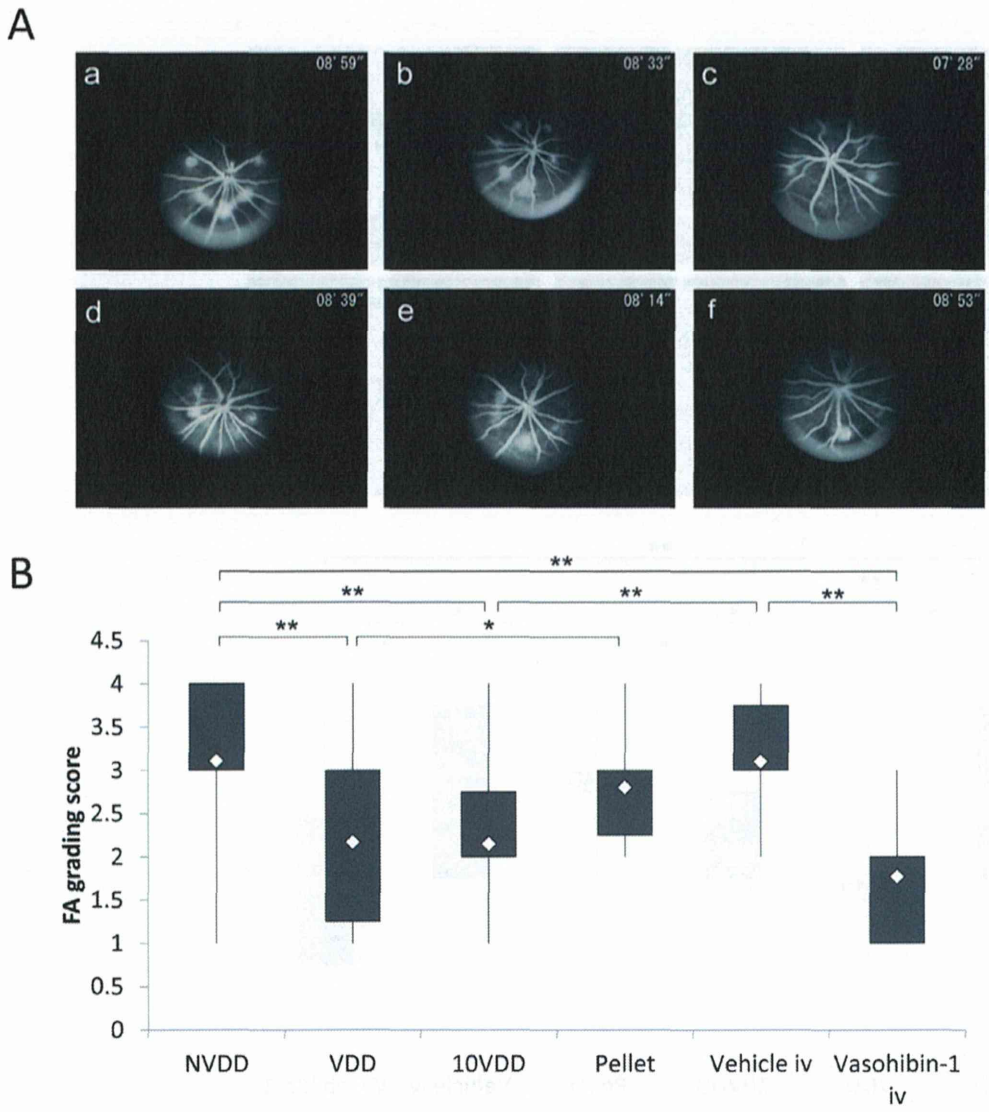

Figure 5. Fluorescein angiography 2 weeks after CNV laser procedure. (A) Representative results of fluorescein angiography in each group at 2 weeks after CNV laser procedure. The groups were treated with NVDD (a), VDD (b), 10VDD (c), vasohibin-1 pellet (d), intravitreal vehicle injection (Vehicle iv) (e), intravitreal vasohibin-1 injection (Vasohibin-1 iv) (f). (B) Significantly lower FA scores was shown in the Vasohibin-1 iv group when compared to those of NVDD ($p = 0.000022$), and Vehicle iv ($p = 0.0065$). Significantly lower FA scores are also observed in the 10VDD group when compared to the NVDD group ($p = 0.00003$) and intravitreal vehicle injection ($p = 0.011$). Significant differences are shown as asterisks. NVDD: non-vasohibin-1 (vehicle) delivery device, VDD: 1 μM vasohibin-1 delivery device, 10VDD: 10 μM vasohibin-1 delivery device, Pellets: vasohibin-1 pelletized at the same concentration of 10VDD (without reservoir and cover).
doi:10.1371/journal.pone.0058580.g005

deviation in the 10VDD group may be indicative of imperfect device preparation. From the results of western blotting, the 10VDD group showed a mild initial release of drug, although the level was far less than seen in the pellet-only group. Technical improvements in delivery device design may overcome these problems. This is an attractive device designed with sustained protein delivery for the treatment of eye diseases.

Subconjunctival drug administration produces better drug penetration than eye drops and is less invasive than intravitreal injection. However, conjunctival and episcleral blood and lymphatic flows have been reported to be the main limiting factors for posterior segment drug distribution by subconjunctival drug administration [38–40]. Our results also showed that implantation of pelletized vasohibin-1 alone (with no reservoir) produced much less vasohibin-1 immunoreactivity than seen with 10VDD implantation. Implanted between the sclera and conjunctiva, our device was designed to release the drugs only to the scleral side of the eye, so a limiting factor of drug diversion to the conjunctival blood flow may be reduced. Carvalho et al [41] reported that their tightly-sutured, one-side-open device delivered higher amount of sodium fluorescein than others, although they used small molecules with their device. From the histological analysis of our experimental procedure, we saw no signs of inflammation or adverse effects in the eye that could be attributed

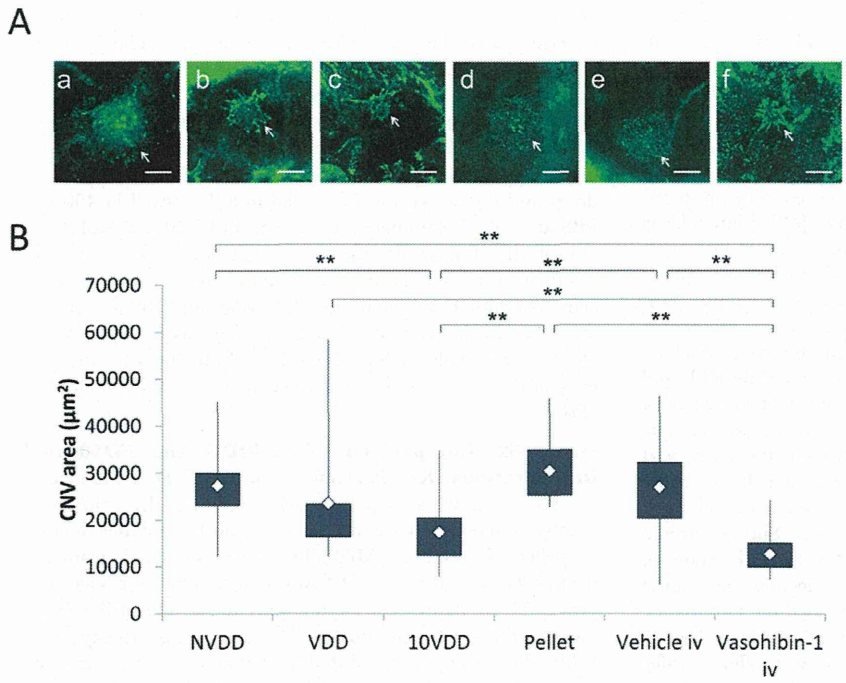

Figure 6. Flat-mount examination of the CNV site. The areas of choroidal neovascularization with devices, pellets, and intravitreal injection of recombinant vasohibin-1 protein. (A) Representative choroidal flat-mount photographs of the groups treated with NVDD (a), VDD (b), 10VDD (c), vasohibin-1 pellet (Pellet) (d), intravitreal vehicle injection (Vehicle iv) (e), intravitreal vasohibin-1 injection (Vasohibin-1 iv) (f) eyes at 2 weeks after the CNV laser procedure. Mean values of actual areas are shown in the text. Bars: 200 μm. (B) Significantly smaller CNV areas were observed in the 10VDD group when compared to those of the NVDD ($p = 0.0004$), Pellet ($p = 0.0011$), and Vehicle iv groups ($p = 0.000015$). Significantly smaller CNV areas were observed in eyes treated with Vasohibin-1 iv when compared to those treated with NVDD ($p = 0.000006$), VDD ($p = 0.0036$), Pellet ($p = 0.000023$), or Vehicle iv ($p = 0.000001$). NVDD: non-vasohibin-1 (vehicle) delivery device, VDD: 1 μM vasohibin-1 delivery device, 10VDD: 10 μM vasohibin-1 delivery device, Pellet: vasohibin-1 pelletized at the same concentration of 10VDD (without reservoir and cover).
doi:10.1371/journal.pone.0058580.g006

to device implantation, except for a mild fibrosis observed around the devices at 2 weeks post-surgery. We also found that the devices removed from the rats where fibrosis was noted showed continuing vasohibin-1 release and comparable activity when we cultured the removed device/tissues in PBS (data not shown).

Vasohibin-1 was observed on the retina at 2 weeks post-implant, principally noted in the regions where the devices were implanted. Some of the regions showed strong immunoreactivity for vasohibin-1, especially at the retinal pigmented epithelium (RPE) and the retinal ganglion cell layer (GCL); the first finding may be due to being the main outer blood-retinal barrier, while the second may be due to the vitreous-retinal barrier [42]. Vasohibin-1 released from the device may be stored in cells in these regions and later released to other regions of the retina or vitreous.

Our results demonstrated that vasohibin-1 can be delivered by our device into the retina transsclerally. Amaral et al also reported transscleral protein (pigment epithelium-derived factor and ovalbumin) delivery into the retina, although they used uncontrollable drug release via a matrix-type implant [10]. Drug released from their device was not delivered unidirectionally. Although there is a blood-retinal barrier, the penetration of such large molecules into the eye may not be so surprising. When we consider the phenomenon of some type of cancer-associated retinopathy, auto-antibodies against retinal cells or retinal-specific antigens have been reported to cause retinal dysfunction [43–45]. The elimination of proteins is reported to be one to two orders of magnitude slower than that of small molecules via the sub-conjunctival and episcleral blood flow [46], with similar results reported for the choroidal blood flow [21]. This fact may also help protein delivery to the retina with the use of our device.

Although we have not studied vasohibin-1 release from the device for more than 2 weeks *in vivo* because of the experimental design, more than 80% of the vasohibin-1 was present in the device at the end of the experimental procedure. The devices removed at the end of the experiment were still releasing vasohibin-1 (data not shown), indicating that it might be possible to use the implanted device for a longer time. These data could also indicate that we may be able to use a smaller device than those used in this experiment to deliver the same amount of drug.

Fluorescein angiography examination showed significantly lower scores in the eyes that received intravitreal vasohibin-1 than those of the intravitreal vehicle-injected eyes. The effects of vasohibin-1 were also confirmed from the flat-mount experiments. These results were same as those previously noted in mice [25]. Our 10VDD device delivered vasohibin-1 to the retina transsclerally, with results comparable to those seen with intravitreal vasohibin-1 injections. With a less invasive method than that of intravitreal injection and the added advantage of continuous drug delivery, our device may be able to replace invasive intravitreal drug injections. Although there was no significant difference between 10VDD and VDD when we evaluated by FA, a statistically significant effect was observed in only 10VDD, but not VDD when we performed the flat-mount examination. One of the reasons these two do not match exactly may be due to the uncertainty about the FA evaluation, as not only blockage by

hemorrhage, but also tissue staining and/or leakage sometimes make evaluation difficult [47]. Further study is needed to determine the exact amounts of vasohibin-1 released from the device, the kinetics of drug distribution, the correlation between drug amount and ocular distribution, and the effects of this regimen on CNV, as well as the appropriate duration of vasohibin-1 release.

Choroidal neovascularization has been reported to be produced by choriocapillaris of the choroidal blood flow [48]. Many effects of choroidal blood flow or RPE may stimulate CNV formation into the retina [49]. Drusen, a preclinical feature of age-related macular degeneration, also stimulates CNV formation [50]. Transscleral anti-CNV drug delivery will be more reasonable than that of intravitreal injection not only from the points of safety, but also from the aspect of CNV pathophysiology. The RPE and RPE-choroid complex are reported to be one to two orders of magnitude slower in drug penetration [21]. When we put our device on the sclera, the drug can pass through the sclera and reach the choroid and RPE earlier than the retina. Between the choroid and neural retina, anti-CNV drugs released from our device may suppress on-going CNV formation. Suprachoroidal bevacizumab was reported to be delivered to the RPE, choroid, and photoreceptors, whereas intravitreal injection distributed more to the inner retina [11]. Olsen et al stressed the importance of delivery of a sustained-release formulation of large molecules to the suprachoroidal space [11]. Our device will offer a safer therapeutic method than those previously reported, especially in the treatment of AMD.

Conclusion

We developed a sustained delivery device for the release of vasohibin-1 in the eye. The released vasohibin-1 showed activity comparable to vasohibin-1 delivered via other methods. When we placed the device on the rat sclera, we found vasohibin-1 released to the sclera, retinal pigment epithelium, and retina. Transscleral vasohibin-1 delivery significantly reduced laser-induced CNV that are comparable as those of effects seen with intravitreal vasohibin-1 injection in the rat eye. Our device will offer a safer therapeutic method than intravitreal injections.

Supporting Information

Figure S1 The size of the devices. The size of the device was 4 mm×4 mm×1.5 mm for the vasohibin-1 releasing assay (A, Device (a)) and 2 mm×2 mm wide ×1 mm high for the rat experiments (A, Device (b)). Because it was very difficult to detect using standard ELISA techniques, we used a larger size device for ELISA. The vasohibin-1 releasing area was 5.44 times larger in Device (a) (3.5 mm×3.5 mm = 12.25 mm^2) than that of Device (b) (1.5 mm×1.5 mm = 2.25 mm^2). Bar: 5 mm. We formulated fluorescein isothiocyanate (FITC) dextran (FD40) as simulated drugs and the device was incubated in a Transwell in 400 μL of PBS at 37°C. To estimate the amounts of FD40 that had diffused out of the Transwells, the fluorescent intensities of the PBS solutions were measured spectrofluorometrically (FluoroscanAscent; Thermo). From the results of a fitting curve (B), we calculated that the releasing rate of the larger device was 0.958 μg/hr/day, whereas the smaller device released 0.28 μg/hr/day; the difference of the releasing rates was calculated as 3.42 (0.958/0.28).
(TIF)

Figure S2 Comparison of FD40DD and FD40 pellet implantations. Rats implanted with FD40DD or FD40 pellets are shown. Devices or pellets were confirmed by color photographs (A and G), after enucleation (C and I), and after device (E) or pellet (K) removal. Mild fibrosis was observed around the devices (C) or pellets (I). FD40 was detected in the device (B), or pellets (H) by fluorescein photography at the site of the implant through the conjunctiva in the live rats during the experiment. When the eyes were enucleated at 1 week after device implantation, little fluorescence was observed in the conjunctiva and surrounding tissues (D, white arrow) in FD40DD-treated rats, whereas strong fluorescence in the conjunctiva was observed in pellet-treated rats (J, white arrow). FD40 was also detected on the sclera after removal of the device (F), but not the pellet (L) (yellow squares indicate the implantation site).
(TIF)

Acknowledgments

The authors alone are responsible for the content and writing of this paper.

Author Contributions

Conceived and designed the experiments: TA NN. Performed the experiments: HO NN HK MN YS NO TN TA. Analyzed the data: HO NN TA. Contributed reagents/materials/analysis tools: NN HK MN TA. Wrote the paper: TA.

References

1. Klein R, Peto T, Bird A, Vannewkirk MR (2004) The epidemiology of age-related macular degeneration. Am J Ophthalmol 137: 486–495.
2. (1986) Argon laser photocoagulation for neovascular maculopathy. Three-year results from randomized clinical trials. Macular Photocoagulation Study Group. Arch Ophthalmol 104: 694–701.
3. Thomas MA, Grand MG, Williams DF, Lee CM, Pesin SR, et al. (1992) Surgical management of subfoveal choroidal neovascularization. Ophthalmology 99: 952–968; discussion 975–956.
4. Eckardt C, Eckardt U, Conrad HG (1999) Macular rotation with and without counter-rotation of the globe in patients with age-related macular degeneration. Graefes Arch Clin Exp Ophthalmol 237: 313–325.
5. Reichel E, Berrocal AM, Ip M, Kroll AJ, Desai V, et al. (1999) Transpupillary thermotherapy of occult subfoveal choroidal neovascularization in patients with age-related macular degeneration. Ophthalmology 106: 1908–1914.
6. (1999) Photodynamic therapy of subfoveal choroidal neovascularization in age-related macular degeneration with verteporfin: one-year results of 2 randomized clinical trials – TAP report. Treatment of age-related macular degeneration with photodynamic therapy (TAP) Study Group. Arch Ophthalmol 117: 1329–1345.
7. Grisanti S, Tatar O (2008) The role of vascular endothelial growth factor and other endogenous interplayers in age-related macular degeneration. Prog Retin Eye Res 27: 372–390.
8. Miller JW, Adamis AP, Shima DT, D'Amore PA, Moulton RS, et al. (1994) Vascular endothelial growth factor/vascular permeability factor is temporally and spatially correlated with ocular angiogenesis in a primate model. Am J Pathol 145: 574–584.
9. Pilli S, Kotsolis A, Spaide RF, Slakter J, Freund KB, et al. (2008) Endophthalmitis associated with intravitreal anti-vascular endothelial growth factor therapy injections in an office setting. Am J Ophthalmol 145: 879–882.
10. Amaral J, Fariss RN, Campos MM, Robison WG Jr., Kim H, et al. (2005) Transscleral-RPE permeability of PEDF and ovalbumin proteins: implications for subconjunctival protein delivery. Invest Ophthalmol Vis Sci 46: 4383–4392.
11. Olsen TW, Feng X, Wabner K, Csaky K, Pambuccian S, et al. (2011) Pharmacokinetics of pars plana intravitreal injections versus microcannula suprachoroidal injections of bevacizumab in a porcine model. Invest Ophthalmol Vis Sci 52: 4749–4756.
12. Martin DF, Parks DJ, Mellow SD, Ferris FL, Walton RC, et al. (1994) Treatment of cytomegalovirus retinitis with an intraocular sustained-release ganciclovir implant. A randomized controlled clinical trial. Arch Ophthalmol 112: 1531–1539.
13. Charles NC, Freisberg L (2002) Endophthalmitis associated with extrusion of a ganciclovir implant. Am J Ophthalmol 133: 273–275.
14. Srivastava S, Taylor P, Wood LV, Lee SS, Robinson MR (2004) Post-surgical scleritis associated with the ganciclovir implant. Ophthalmic Surg Lasers Imaging 35: 254–255.

15. Cashman SM, Ramo K, Kumar-Singh R (2011) A non membrane-targeted human soluble CD59 attenuates choroidal neovascularization in a model of age related macular degeneration. PLoS One 6: e19078.
16. Campochiaro PA, Nguyen QD, Shah SM, Klein ML, Holz E, et al. (2006) Adenoviral vector-delivered pigment epithelium-derived factor for neovascular age-related macular degeneration: results of a phase I clinical trial. Hum Gene Ther 17: 167–176.
17. Chevez-Barrios P, Chintagumpala M, Mieler W, Paysse E, Boniuk M, et al. (2005) Response of retinoblastoma with vitreous tumor seeding to adenovirus-mediated delivery of thymidine kinase followed by ganciclovir. J Clin Oncol 23: 7927–7935.
18. Raghava S, Hammond M, Kompella UB (2004) Periocular routes for retinal drug delivery. Expert Opin Drug Deliv 1: 99–114.
19. Smiddy WE, Smiddy RJ, Ba'Arath B, Flynn HW Jr., Murray TG, et al. (2005) Subconjunctival antibiotics in the treatment of endophthalmitis managed without vitrectomy. Retina 25: 751–758.
20. Yasukawa T, Ogura Y, Tabata Y, Kimura H, Wiedemann P, et al. (2004) Drug delivery systems for vitreoretinal diseases. Prog Retin Eye Res 23: 253–281.
21. Ranta VP, Mannermaa E, Lummepuro K, Subrizi A, Laukkanen A, et al. (2010) Barrier analysis of periocular drug delivery to the posterior segment. J Control Release 148: 42–48.
22. Kunou N, Ogura Y, Yasukawa T, Kimura H, Miyamoto H, et al. (2000) Long-term sustained release of ganciclovir from biodegradable scleral implant for the treatment of cytomegalovirus retinitis. J Control Release 68: 263–271.
23. McHugh AJ (2005) The role of polymer membrane formation in sustained release drug delivery systems. J Control Release 109: 211–221.
24. Kawashima T, Nagai N, Kaji H, Kumasaka N, Onami H, et al. (2011) A scalable controlled-release device for transscleral drug delivery to the retina. Biomaterials 32: 1950–1956.
25. Wakusawa R, Abe T, Sato H, Sonoda H, Sato M, et al. (2011) Suppression of choroidal neovascularization by vasohibin-1, a vascular endothelium-derived angiogenic inhibitor. Invest Ophthalmol Vis Sci 52: 3272–3280.
26. Watanabe K, Hasegawa Y, Yamashita H, Shimizu K, Ding Y, et al. (2004) Vasohibin as an endothelium-derived negative feedback regulator of angiogenesis. J Clin Invest 114: 898–907.
27. Shen J, Yang X, Xiao WH, Hackett SF, Sato Y, et al. (2006) Vasohibin is up-regulated by VEGF in the retina and suppresses VEGF receptor 2 and retinal neovascularization. FASEB J 20: 723–725.
28. Onami H, Nagai N, Machida S, Kumasaka N, Wakusawa R, et al. (2012) Reduction of laser-induced choroidal neovascularization by intravitreal vasohibin-1 in monkey eyes. Retina 32: 1204–1213.
29. Heishi T, Hosaka T, Suzuki Y, Miyashita H, Oike Y, et al. (2010) Endogenous angiogenesis inhibitor vasohibin1 exhibits broad-spectrum antilymphangiogenic activity and suppresses lymph node metastasis. Am J Pathol 176: 1950–1958.
30. Ishikawa Y, Nagai N, Onami H, Kumasaka N, Wakusawa R, et al. (2012) Vasohibin-1 and retinal pigment epithelium. Adv Exp Med Biol 723: 305–310.
31. Tobe T, Ortega S, Luna JD, Ozaki H, Okamoto N, et al. (1998) Targeted disruption of the FGF2 gene does not prevent choroidal neovascularization in a murine model. Am J Pathol 153: 1641–1646.
32. Krzystolik MG, Afshari MA, Adamis AP, Gaudreault J, Gragoudas ES, et al. (2002) Prevention of experimental choroidal neovascularization with intravitreal anti-vascular endothelial growth factor antibody fragment. Arch Ophthalmol 120: 338–346.
33. Yu HG, Liu X, Kiss S, Connolly E, Gragoudas ES, et al. (2008) Increased choroidal neovascularization following laser induction in mice lacking lysyl oxidase-like 1. Invest Ophthalmol Vis Sci 49: 2599–2605.
34. Edelman JL, Castro MR (2000) Quantitative image analysis of laser-induced choroidal neovascularization in rat. Exp Eye Res 71: 523–533.
35. Regillo CD, Brown DM, Abraham P, Yue H, Ianchulev T, et al. (2008) Randomized, double-masked, sham-controlled trial of ranibizumab for neovascular age-related macular degeneration: PIER Study year 1. Am J Ophthalmol 145: 239–248.
36. Sfikakis PP, Theodossiadis PG, Katsiari CG, Kaklamanis P, Markomichelakis NN (2001) Effect of infliximab on sight-threatening panuveitis in Behcet's disease. Lancet 358: 295–296.
37. Ohno S, Nakamura S, Hori S, Shimakawa M, Kawashima H, et al. (2004) Efficacy, safety, and pharmacokinetics of multiple administration of infliximab in Behcet's disease with refractory uveoretinitis. J Rheumatol 31: 1362–1368.
38. Kim H, Csaky KG (2010) Nanoparticle-integrin antagonist C16Y peptide treatment of choroidal neovascularization in rats. J Control Release 142: 286–293.
39. Robinson MR, Lee SS, Kim H, Kim S, Lutz RJ, et al. (2006) A rabbit model for assessing the ocular barriers to the transscleral delivery of triamcinolone acetonide. Exp Eye Res 82: 479–487.
40. Lee SJ, He W, Robinson SB, Robinson MR, Csaky KG, et al. (2010) Evaluation of clearance mechanisms with transscleral drug delivery. Invest Ophthalmol Vis Sci 51: 5205–5212.
41. Pontes de Carvalho RA, Krausse ML, Murphree AL, Schmitt EE, Campochiaro PA, et al. (2006) Delivery from episcleral exoplants. Invest Ophthalmol Vis Sci 47: 4532–4539.
42. Stefansson E, Geirsdottir A, Sigurdsson H (2011) Metabolic physiology in age related macular degeneration. Prog Retin Eye Res 30: 72–80.
43. Kondo M, Sanuki R, Ueno S, Nishizawa Y, Hashimoto N, et al. (2011) Identification of autoantibodies against TRPM1 in patients with paraneoplastic retinopathy associated with ON bipolar cell dysfunction. PLoS One 6: e19911.
44. Thirkill CE, FitzGerald P, Sergott RC, Roth AM, Tyler NK, et al. (1989) Cancer-associated retinopathy (CAR syndrome) with antibodies reacting with retinal, optic-nerve, and cancer cells. N Engl J Med 321: 1589–1594.
45. Chan JW (2003) Paraneoplastic retinopathies and optic neuropathies. Surv Ophthalmol 48: 12–38.
46. Kim SH, Csaky KG, Wang NS, Lutz RJ (2008) Drug elimination kinetics following subconjunctival injection using dynamic contrast-enhanced magnetic resonance imaging. Pharm Res 25: 512–520.
47. Lassota N, Kiilgaard JF, la Cour M, Scherfig E, Prause JU (2008) Natural history of choroidal neovascularization after surgical induction in an animal model. Acta Ophthalmol 86: 495–503.
48. Hayreh SS (2010) Submacular choroidal vascular bed watershed zones and their clinical importance. Am J Ophthalmol 150: 940–941; author reply 941–942.
49. Lutty G, Grunwald J, Majji AB, Uyama M, Yoneya S (1999) Changes in choriocapillaris and retinal pigment epithelium in age-related macular degeneration. Mol Vis 5: 35.
50. Booij JC, Baas DC, Beisekeeva J, Gorgels TG, Bergen AA (2010) The dynamic nature of Bruch's membrane. Prog Retin Eye Res 29: 1–18.

Neurobiology of Disease 48 (2012) 556–567

Contents lists available at SciVerse ScienceDirect

Neurobiology of Disease

journal homepage: www.elsevier.com/locate/ynbdi

Metabolic stress response implicated in diabetic retinopathy: The role of calpain, and the therapeutic impact of calpain inhibitor

Ahmed Y. Shanab [a], Toru Nakazawa [a,*], Morin Ryu [a], Yuji Tanaka [a], Noriko Himori [a], Keiko Taguchi [b], Masayuki Yasuda [a], Ryo Watanabe [a], Jiro Takano [c], Takaomi Saido [c], Naoko Minegishi [b], Toshio Miyata [d], Toshiaki Abe [e], Masayuki Yamamoto [b]

[a] Department of Ophthalmology, Tohoku University Graduate School of Medicine, Japan
[b] Department of Medical Biochemistry, Tohoku University Graduate School of Medicine, Japan
[c] RIKEN Brain Science Institute, Laboratory for Proteolytic Neuroscience, Japan
[d] Division of Molecular Therapy, Tohoku University Graduate School of Medicine, Japan
[e] Division of Clinical Cell Therapy, Tohoku University Graduate School of Medicine, Japan

ARTICLE INFO

Article history:
Received 13 March 2012
Revised 12 July 2012
Accepted 25 July 2012
Available online 9 August 2012

Keywords:
Diabetic retinopathy
Retinal ganglion cell
Calpain
Oxidative stress
Synaptophysin
Neuroprotection

ABSTRACT

To describe how a high fat diet (HFD) and hyperglycemia initiate a sequence of calpain activation and oxidative stress associated with neuro-degenerative changes in diabetic retinopathy (DR), hyperglycemia was induced with streptozotocin in mice lacking the gene for calpastatin (CAST KO), and in mice lacking the gene for the transcription factor NF-E2 related factor 2 (Nrf2 KO). All animals were fed a HFD. Retinal ganglion cell (RGC) density was estimated by labeling with fluorogold and immunohistochemistry. A potent calpain inhibitor, SNJ-1945, was administered daily until the animals were sacrificed. In vitro, oxidative stress-induced RGC loss was evaluated in a high glucose culture medium with and without SNJ-1945. Retinal mRNA of calpain-1 and calpain-2 was measured by quantitative RT-PCR. Pre-apoptotic substrates of cleaved α-fodrin and synaptophysin protein were quantified by immunoblot analysis. Axonal damage was examined in transverse sections of the optic nerve. A HFD and hyperglycemia significantly increased RGC and axonal degeneration 3 weeks into the experiment. Levels of cleaved α-fodrin were increased. In the CAST KO mice, the neurotoxicity was augmented significantly. Gene manipulation of CAST and orally administered SNJ-1945 successfully modified calpain levels in the retina and prevented RGC death. In vitro, a high-glucose culture of retinal cells without antioxidants showed more RGC death than that with antioxidant treatment. The expression of synaptophysin was significantly suppressed by SNJ-1945 treatment. These results suggest that calpain plays a crucial role in metabolic-induced RGC degeneration caused by hyperglycemia and oxidative stress. Antioxidant and calpain inhibition offers important opportunities for future neuroprotective treatment against RGC death in various metabolic stress-induced diseases including DR.

Introduction

Diabetes mellitus (DM) affects approximately 285 million individuals worldwide (Shaw et al., 2010), and in developing countries, over 95% of all cases are type 2 diabetes (Hu, 2011). Around 21% of those patients will have some kind of retinopathy at the first time of diagnosis (Fong et al., 2004). Despite years of clinical and laboratory investigations, diabetic retinopathy (DR) remains the leading cause of blindness among diabetic patients (Resnikoff et al., 2004). Clinical diagnosis of DR still requires detection of vascular pathology, but there is clear evidence that hyperglycemia can cause abnormal neurological manifestations after only 2-weeks (Hancock and Kraft, 2004; Kizawa et al., 2006).

In the clinic, the amplitude of photopic negative response (PhNR), elicited by weak stimuli under dark-adapted conditions and driven mainly by retinal ganglion cells (RGCs) (Frishman et al., 1996), is reduced among diabetic patients, correlated with the degree of optic nerve damage (Kizawa et al., 2006). Measuring the thickness of circumpapillary retinal nerve fiber layer (cpRNFL), which serves as an index for the viability of RGC, with optical coherence topography (OCT), has also been noted to thin with the progress of DR (Costa et al., 2002). Furthermore, asymmetry of the cpRNFL has been observed by OCT in type 2 diabetes patients with no detectable ophthalmoscopical retinopathy (Chihara et al., 1993). At the cellular level, RGCs in postmortem human diabetic retinas have shown increased markers of apoptosis (Abu-El-Asrar et al., 2004). Taken together, this evidence shows that RGCs undergo apoptosis in

* Corresponding author at: Tohoku University Graduate School of Medicine, Department of Ophthalmology, 1-1 Seiryo, Aoba, Sendai, Miyagi 980-8574, Japan. Fax: +81 22 717 7298.
E-mail address: ntoru@oph.med.tohoku.ac.jp (T. Nakazawa).
Available online on ScienceDirect (www.sciencedirect.com).

0969-9961/$ – see front matter © 2012 Elsevier Inc. All rights reserved.
http://dx.doi.org/10.1016/j.nbd.2012.07.025